

Self-Propagating Eddies on the Stratified f Plane

TIMOUR RADKO AND MELVIN E. STERN

Department of Oceanography, The Florida State University, Tallahassee, Florida

(Manuscript received 23 February 1998, in final form 17 February 2000)

ABSTRACT

Analytical solutions of the shallow-water system of equations in a $1\frac{1}{2}$ -layer f -plane model are obtained for stable quasi-monopolar vortices propagating due to a dipolar (azimuthal mode $m = 1$) component whose amplitude is small compared to the circularly symmetric ($m = 0$) part. The ability of the f -plane eddies with $O(1)$ Rossby number to propagate distances greater than their size is demonstrated by finite amplitude numerical calculations. Numerical and analytical considerations also indicate that significant departures may occur between the “centroid of mass anomaly” (commonly used in theoretical estimates of the speed of oceanic vortices) and other measures of the eddy center.

1. Introduction

The two commonly recognized mechanisms of eddy propagation are advection by an ambient larger-scale motion and the effect of the gradient of planetary vorticity (the so called β effect). The latter produces the small dipolar moment ($m = 1$ circular mode) necessary for the propagation (Flierl 1988; Killworth 1983, 1986; among others). However, such an $m = 1$ mode may be generated in the interactions of the eddies with topography, boundaries, or currents (see Stern and Radko 1998, SR98 hereafter), or it may be produced, along with other Fourier components, in the same process that generated the eddy. In order to distinguish the motion caused by the β effect from the mechanism of propagation due to a more generally produced $m = 1$ mode, the latter will be referred to as the *self-propagation* effect. The simplest example of this effect appears in the barotropic model (SR98), which is now extended to the case of an f -plane shallow water $1\frac{1}{2}$ -layer model.

We use a perturbation theory, in which the amplitude of the $m = 1$ mode is assumed to be small, to construct stable *quasi-monopolar* solutions with large angular and small propagation velocity. For this steady-state theory the question arises as to the period of its validity, since the neglected nonlinear terms and the neglected diffusion of the (assumed) vorticity discontinuity will eventually modify the structure. The same question appeared in our previous work (SR), where we found that a *bar-*

otropic eddy can propagate many radii away from its origin. This was verified both by a weakly nonlinear expansion and by spectral calculations with small viscosity. Likewise, in this paper the ability of the analytical $m = 1$ mode to propel a shallow water eddy over a distance larger than its radius will be verified by numerical calculations initiated with the linear solution.

Oceanic eddies often propagate with velocities that differ significantly, both in magnitude and direction, from what is predicted by the earlier β -plane theories (e.g., Nof 1983). Various effects have been considered to explain the propagation rates that disagree with the theory. For example, Killworth (1986) discovered that in models with a more sophisticated representation of the stratification the eddy can move faster than previously expected. The influence of advection by mean flow was also examined. Yet, so far there is no generally accepted and convincing explanation of a common disagreement between the theory and observations. We suggest (section 8) that the initially introduced small dipolar moment (of nonbeta origin) can significantly affect and, in certain cases, even dominate the propagation velocity for a long time.

It should also be mentioned that because of the complexity of the primitive shallow-water equations most theories for propagating eddies [such as β -plane models of Flierl et al. (1980) or Nycander and Sutyrin (1992)] only consider the case of small Rossby number ($Ro \ll 1$). On the other hand, we demonstrate in section 5 that the effect of *self-propagation* is stronger when the Rossby number is large. The analytical tractability of this problem is achieved by using the primitive equations in the interior of the eddy while taking advantage of the quasigeostrophic approximation in the exterior (only) where the thickness variation is relatively small. Such

Corresponding author address: Dr. Timour Radko, Department of Oceanography, The Florida State University, Tallahassee, FL 32306-4320.

E-mail: radko@ocean.fsu.edu

a melding of the shallow-water and the quasigeostrophic dynamics also prevents the far-field radiation of gravity waves in the analytical model, thereby allowing us to isolate the long-range propagation effect without introducing significant errors in the model.

Our work is connected to the β -plane studies of Nylander and Sutyrin (1992) and Benilov (1996), which recognize the importance of a small dipolar departure from axial symmetry for the westward drift of eddies. However, the mechanism of propagation described by those authors is quite different from ours since the former depends fundamentally on the β effect. Some of the previous studies of the β -induced motion create the unwanted impression that (aside from advection) eddies cannot move at all if $\beta = 0$, and this point is clarified in the present paper.

The quasi-monopolar eddies considered herein should also be distinguished from the strong dipolar vortices, such as Lamb-Batchelor solution or the β -plane “modons” (Larichev and Reznik 1976), which have a dominant $m = 1$ mode and no azimuthal flow. The reader is also referred to Radko and Stern (1999) for a more complete discussion of the theories of isolated quasi-monopolar eddies, and for the connection between the self-propagation effect and the westward motion on the β plane.

2. Formulation

Consider a compact eddy of radius R , with a dominant $m = 0$ circular mode and a small $m = 1$ component, and assume that the entire eddy moves rectilinearly in the x direction. In the following perturbation theory the $m = 0$ mode is cyclostrophically balanced, while both the amplitude of the $m = 1$ mode and the propagation velocity are assumed to be small first-order quantities.

When the primitive shallow-water equations for the upper active layer are nondimensionalized using the eddy radius R as the horizontal length scale, the maximum advective velocity (v_{\max}) of the undisturbed vortex as the velocity scale, and the far-field depth of the upper layer H as the thickness scale, the result is

$$\left. \begin{aligned} \mathbf{u}_t + \mathbf{u} \cdot \nabla \mathbf{u} + F \mathbf{k} \times \mathbf{u} &= -G \nabla h \\ h_t + \nabla \cdot (\mathbf{u} h) &= 0 \end{aligned} \right\}, \quad (1)$$

where $F = fR/v_{\max}$ is the inverse Rossby number, $G = g'H/v_{\max}^2$, $\bar{\mathbf{u}} = (u_x, u_y)$ is the horizontal velocity, and $h(x, y, t)$ is the thickness of the upper layer.

These equations are rewritten below in a coordinate system moving in the x direction with the (nondimensional) velocity U , in which the eddy is assumed to be steady, that is, $\partial/\partial t = 0$. In polar coordinates (r, θ) given by $x = r \cos \theta$, $y = r \sin \theta$, Eq. (1) becomes

$$\left. \begin{aligned} u \frac{\partial u}{\partial r} + \frac{v}{r} \frac{\partial u}{\partial \theta} - \frac{v^2}{r} - F(v - U \sin \theta) &= -G \frac{\partial h}{\partial r} \\ u \frac{\partial v}{\partial r} + \frac{v}{r} \frac{\partial v}{\partial \theta} + \frac{uv}{r} + F(u + U \cos \theta) &= -\frac{1}{r} G \frac{\partial h}{\partial \theta} \\ \frac{\partial(hv)}{\partial \theta} + \frac{\partial(rhv)}{\partial r} &= 0 \end{aligned} \right\}, \quad (2)$$

where u and v are radial and azimuthal velocities in the moving system (i.e., these velocities do not vanish at $r \rightarrow \infty$). In the basic circularly symmetric state ($m = 0$) the azimuthal velocity \bar{v} and the upper layer thickness \bar{h} are cyclostrophically balanced:

$$\frac{\bar{v}^2}{r} + F\bar{v} = G \frac{\partial \bar{h}}{\partial r} \quad (3)$$

with $\bar{v} = 0$ and constant $\bar{h} = 1$ in the exterior ($r > 1$) of the eddy.

When (2) is linearized assuming that the radially symmetric part is much larger than the dipolar component in the interior $r < 1$, and when the variables are separated using

$$\left. \begin{aligned} u &= \hat{u}(r) \cos \theta \\ v &= \bar{v}(r) + \hat{v}(r) \sin \theta \\ h &= \bar{h}(r) + \hat{h}(r) \sin \theta \end{aligned} \right\}, \quad (4)$$

where $\langle \hat{v} \rangle \sim \langle \hat{u} \rangle \sim \langle \hat{h} \rangle \sim U \sim \varepsilon \ll 1$, the result is

$$\left. \begin{aligned} \left(\frac{\bar{v} \hat{v}}{r} + \hat{u} \frac{\partial \bar{v}}{\partial r} + \frac{\hat{u} \bar{v}}{r} \right) + F(\hat{u} + U) &= -G \frac{\hat{h}}{r} \\ \left(-\frac{\bar{v} \hat{u}}{r} - \frac{2\bar{v} \hat{v}}{r} \right) - F(\hat{v} - U) &= -G \frac{\partial \hat{h}}{\partial r} \\ \frac{\partial}{\partial r}(r \bar{h} \hat{u}) + \bar{h} \hat{v} + \hat{h} \bar{v} &= 0 \end{aligned} \right\}. \quad (5)$$

As indicated earlier, a much simpler set of equations will apply to the exterior ($r > 1$) field where depth perturbations are small.

3. Case of a ($f = 0$)

The simplest, and perhaps the most fundamental physical case, $f = 0 = F$, is considered first; the resulting theory will provide us with insight into the more general rotational problem (sections 5, 6). The $f = 0$ case is also of direct interest for vortices whose scale is much smaller than the Rossby radius of deformation. Furthermore, this is one of the cases for which the integral theorems (Ball 1963) allow uniform propagation, and therefore a rigorous solution of the linearized problem is likely to exist.

Since the basic velocity $\bar{v}(r)$ is assumed to be zero in the exterior ($r \geq 1$), the total velocities are of order

$O(\varepsilon)$, so the acceleration and therefore the depth perturbations (\hat{h}) for $r \geq 1$ are at most $O(\varepsilon^2)$. [Scaling of the pressure as $O(\varepsilon^2)$ follows also from the Bernoulli invariant in which velocities are $O(\varepsilon)$ in the exterior.] The leading order $O(\varepsilon)$ approximation of the continuity equation in (1) then yields a nondivergent velocity field, which can be described by the streamfunction $\psi = O(\varepsilon)$, and $v = \partial\psi/\partial r$; $u = -r^{-1}\partial\psi/\partial\theta$. For the same reasons ($\hat{h} \sim \varepsilon^2$) it follows from potential vorticity conservation that at $O(\varepsilon)$ the exterior flow perturbation may be taken to be irrotational. In this case there exists a well-known potential solution corresponding to a flow around a unit circle (recall that our theory assumes a continuous velocity across the $r = 1$ circle with $\hat{u}(1^-) = \hat{u}(1^+) = 0$ for the normal component):

$$\begin{aligned} \psi &= U\left(r - \frac{1}{r}\right) \sin\theta; & \hat{v} \sin\theta &= \frac{\partial\psi}{\partial r}, \\ \hat{u} \cos\theta &= -\frac{1}{r} \frac{\partial\psi}{\partial\theta}, & \hat{h} &= 0 \quad \text{for } r > 1 \end{aligned}$$

and therefore the (continuous) azimuthal velocity at $r = 1$ is $\hat{v}(1^-) = \partial\psi/\partial r = 2U$.

The continuity of the depth ($\hat{h}(1^-) = \hat{h}(1^+) = 0$) then will be satisfied automatically, as can be seen from the interior equations:

$$\left. \begin{aligned} \frac{\bar{v}\hat{v}}{r} + \hat{u}\frac{\partial\bar{v}}{\partial r} + \frac{\hat{u}\bar{v}}{r} &= -G\frac{\hat{h}}{r} \\ \frac{\bar{v}\hat{u}}{r} + \frac{2\bar{v}\hat{v}}{r} &= G\frac{\partial\hat{h}}{\partial r} \\ \frac{\partial}{\partial r}(r\bar{h}\hat{u}) + \bar{h}\hat{v} + \hat{h}\bar{v} &= 0 \end{aligned} \right\}, \quad r < 1, \quad (6)$$

which are obtained from (5) by setting $F = 0$. In addition to the boundary conditions $\hat{v}(1) = 2U$, $\hat{u}(1) = 0$ at $r = 1$, it is important to keep in mind that the cyclostrophic relationship (3) for the basic field now reduces to

$$\begin{aligned} \frac{\bar{v}^2}{r} &= G\frac{\partial\bar{h}}{\partial r}, & r < 1 \\ \bar{v}(r) &= 0, \quad \bar{h}(r) = 1, & r \geq 1. \end{aligned} \quad (7)$$

Direct substitution shows that when (7) is satisfied one solution of (6) with $\hat{u}(1) = 0$ is

$$\left. \begin{aligned} \hat{u} &= -\alpha\frac{\bar{v}}{r} \\ \hat{v} &= \alpha\frac{\partial\bar{v}}{\partial r} \\ \hat{h} &= \alpha\frac{\partial\bar{h}}{\partial r} \end{aligned} \right\}, \quad r < 1 \quad (8a)$$

and the $\hat{v}(1) = 2U$ boundary condition is satisfied if

$$\alpha = \frac{2U}{\bar{v}'(1)}. \quad (8b)$$

The leading order exterior field is given by

$$\left. \begin{aligned} \hat{h}(r) &= 0 \\ \hat{v}(r) &= U\left(1 + \frac{1}{r^2}\right) \\ \hat{u}(r) &= U\left(-1 + \frac{1}{r^2}\right) \end{aligned} \right\}, \quad r > 1. \quad (8c)$$

Thus for any G and any given (small) U we can find at least one solution (8a,b,c) for a rectilinearly propagating eddy provided that the basic vortex is in cyclostrophic balance, has zero basic velocity, and has nonzero vorticity at the edge ($r = 1^-$).

The foregoing expression for the interior solution (8a) implies that all the structure inside the $r = 1$ circle is displaced by the same small distance perpendicular to the direction of the propagation. Reference is made to Benilov (1996), who notes that disturbances like (8a), but which occupy the entire (x, y) plane, simply produce a uniform Galilean shift of the entire eddy; this is equivalent to merely redefining the origin of a coordinate system. In our case, however, there is a real structural distortion of the eddy resulting in a *dynamical* effect: only a part of the flow ($r < 1$) is uniformly displaced in the y direction and the exterior ($r > 1$) is still symmetric with respect to the $y = 0$ axes; this results in a dipolar moment that propels the eddy in x direction. The shift of interior allows us to match velocities at the circular boundary with the dipolar exterior. Similar structures have been found in the barotropic (SR) and in the equivalent barotropic (Radko and Stern 1999) models, where the structure is referred to as an ‘‘alpha-gyre.’’

The value of the dimensional propagation velocity U_{dim} , obtained by integrating the last equation of (8a) over the interval $0 < r < 1$ and returning to the dimensional variables, is

$$U_{\text{dim}} = \frac{1}{2} \frac{\int_0^R h_{\text{pert}} dr}{H - \bar{h}_{\text{dim}}(0)} \cdot \frac{\partial\bar{v}_{\text{dim}}}{\partial r} \Big|_{r=R} \approx \frac{\int_0^R h_{\text{pert}} dr}{H - \bar{h}_{\text{dim}}(0)} \frac{v_{\text{max}}}{R},$$

where h_{pert} is the dimensional deviation (measured positive downward) of the thermocline depth from the circularly symmetric state, $\bar{h}_{\text{dim}}(0)$ is the total depth at the center of the eddy, and maximum azimuthal velocity v_{max} is assumed to occur approximately at the distance $R/2$ from the center.

A plot of our solution is presented in Fig. 1 for $G = 5$, $U = 0.1$ and for the undisturbed state given by (9a,b) in section 4. The contour intervals in the area of the cyclonic rotation where $h < 1$ (upper part of the vortex) are 0.05, while in the area of anticyclonic rotation (lower

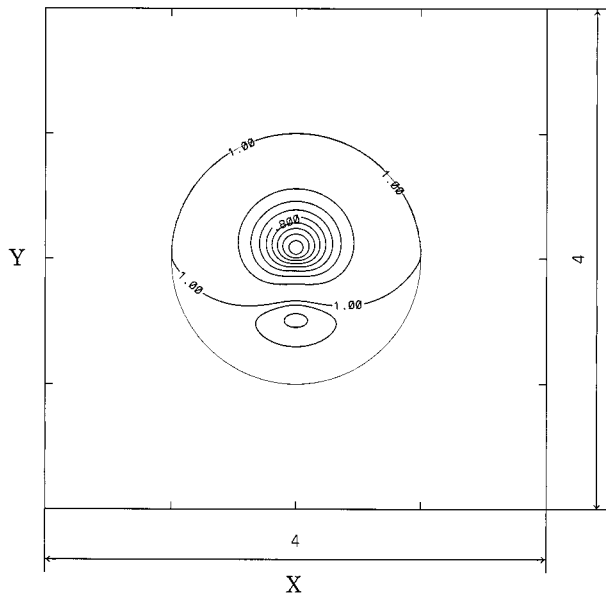


FIG. 1. Isopleths of the upper-layer thickness for the analytical solution with zero value of the Coriolis force, $G = 5$. The contour interval is 0.05 for the cyclonic (upper) part of the eddy where $h < 1$ and 0.005 for the anticyclonic (lower) part of the eddy where $h > 1$. This reflects the extremely weak expression of the anticyclonic companion in terms of the thickness variation. A small dipolar component, however, causes a significant dynamical effect. The maximum variation in the thickness of the active upper layer are comparable to its far-field depth. The vortex is moving uniformly to the right (see the text).

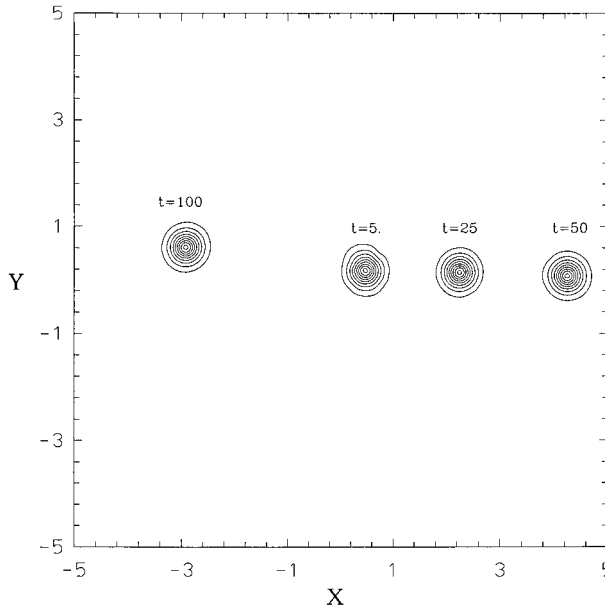


FIG. 2. Numerical simulation of the evolution of the reduced-gravity vortex in Fig. 1. Calculations were initiated by the analytical theory of section 3, and the doubly periodic boundary conditions are used for the integration. Results are displayed in isobar contours for $t = 5, 25, 50,$ and 100 for experimental parameters $G = 5$, Coriolis parameter zero, and analytical propagation velocity $U = 0.1$. The vortex propagates in the $+x$ direction with the velocity close to the theoretical speed. A slight deflection of the trajectory to its left can be observed at the late stages of the experiment. The contour interval is equal to 0.05.

part of the vortex) these are 0.005. Thus the extremely small depression of the density interface in the anticyclonic part might be difficult to detect in field measurements; that is, the whole eddy looks like a monopolar structure.

4. Numerical calculations for the $f = 0$ case

In order to determine the extent to which the foregoing solution is realizable in the sense of an initial value calculation, we used the Bleck and Boudra (1986) reduced-gravity 1½-layer finite difference C-grid numerical model. A small Laplacian dissipational term with the nondimensional viscosity $\nu = 5 \times 10^{-9}$ was added to the right-hand side of the two-dimensional shallow-water equations [first equation of (1)] to control the numerical stability of the code, and periodic boundary conditions in both x and y were prescribed on the boundaries of the computational domain. The following calculations have been made on a 256×256 grid with space increments $\Delta x = \Delta y = 0.04$ with a leapfrog time step $\Delta t = 0.001$.

The calculations for $G = 3, 5, 10$ were made in a stationary coordinate system and the code was initiated by the linear theory of section 3 with the basic velocity profile

$$\bar{v} = 8.65r(1 - r) \exp(-2r), \quad r < 1. \quad (9a)$$

The coefficient 8.65 is included in order to comply with the nondimensionalization (see sec. 2) that sets the maximum of the basic velocity to 1. The term $\exp(-2r)$ is used here for stability considerations (Flierl 1988), which suggest that circular vortices are stable if the inner region of (say) positive vorticity is sufficiently small compared to the vortex radius. The corresponding undisturbed depth is

$$\bar{h} = \frac{8.65^2}{G} \left[\left(-\frac{3}{128} - \frac{3}{32}r + \frac{5}{16}r^2 - \frac{1}{4}r^3 \right) \exp(-4r) + \frac{7}{128} \exp(-4) \right] + 1, \quad r < 1. \quad (9b)$$

We used $G = 5$ for which the undisturbed depth at the center of the (cyclonic) vortex is 0.67; therefore it is clear that the primitive shallow-water equations, rather than the two-dimensional equations, must be used in the interior of this eddy. Initial perturbation velocities and depth were computed using (8a,c) in which α was obtained from (8b) for $U = 0.1$; the total velocities were then given by (4).

The results of the $G = 5$ experiment (Fig. 2) show that by time $t = 70$ the vortex covered a distance of 7 radii, and this propagation velocity is in agreement with the foregoing linear value of $U = 0.1$. The $h = 1$ isopleth

(not shown) indicates the existence of irregular disturbances which result from the fast gravity waves excited by higher order nonlinear terms (not taken into account in our linear theory) and by artificial boundary conditions. Nevertheless, our vortex is robust enough to preserve its initial direction, velocity, and initial structure for 70 nondimensional time units. After that the ($m = 1$) initial state of our eddy is gradually destroyed, the propagation velocity decreases, and the dipolar component of the vortex is rotated by the basic cyclonic flow causing the vortex to turn gradually to its left (see the $t = 100$ vortex in Fig. 2). A vortex propagating uniformly for *all* time is not to be expected because of the radiation of gravity waves. The experiments with $G = 3$ and $G = 10$ (not shown) resulted in approximately the same distances for the rectilinear propagation. We regard this primitive solution as being of fundamental physical interest in vortex dynamics.

5. Effects of finite Coriolis force

We now turn to the case ($f \neq 0$) of greater oceanographic interest. For reasons of analytical tractability it is convenient to introduce a function

$$\Phi = \hat{h} + \frac{FU}{G}r,$$

and then Eqs. (5) reduce to

$$\left. \begin{aligned} \left(\frac{\bar{v}\hat{v}}{r} + \hat{u}\frac{\partial\bar{v}}{\partial r} + \frac{\hat{u}\bar{v}}{r} \right) + F\hat{u} &= -G\frac{\Phi}{r} \\ \left(\frac{\bar{v}\hat{u}}{r} + \frac{2\bar{v}\hat{v}}{r} \right) + F\hat{v} &= G\frac{\partial\Phi}{\partial r}, \quad r < 1. \\ \frac{\partial}{\partial r}(r\bar{h}\hat{u}) + \bar{h}\hat{v} + \Phi\bar{v} - \frac{FU}{G}\bar{v}r &= 0 \end{aligned} \right\} \tag{10}$$

As previously mentioned we use the quasigeostrophic approximation in the outer $r > 1$ region so that the nondivergent perturbation velocities are expressible in terms of a streamfunction Ψ :

$$\hat{v} \sin\theta = \frac{\partial\Psi}{\partial r}, \quad \hat{u} \cos\theta = -\frac{1}{r} \frac{\partial\Psi}{\partial\theta}.$$

In this uniform potential vorticity region ($r > 1$) there exists a well-known exact quasi-geostrophic solution with zero potential vorticity, and the corresponding streamfunction (in the moving coordinate system) is

$$\psi = U \left(r - \frac{K_1\left(\frac{r}{R_d}\right)}{K_1\left(\frac{1}{R_d}\right)} \right) \sin\theta, \quad r > 1,$$

where K_1 is the modified Bessel function and

$$R_d = \frac{(g'H)^{1/2}}{fR} = \frac{G^{1/2}}{F}$$

is the nondimensional Rossby radius of deformation. According to the quasigeostrophic approximation the elevation of the density interface is

$$\hat{h}(r) = -\frac{FU}{G} \frac{K_1\left(\frac{r}{R_d}\right)}{K_1\left(\frac{1}{R_d}\right)}$$

for $r > 1$.

The boundary conditions on the interior solution require zero normal velocity [$\hat{u}(1^-) = 0$] and continuity of the azimuthal velocity,

$$\hat{v}(1^-) = \frac{\partial\psi}{\partial r}\Big|_{1^-} = U \left(1 + \frac{K_0\left(\frac{1}{R_d}\right) + K_2\left(\frac{1}{R_d}\right)}{2R_d K_1\left(\frac{1}{R_d}\right)} \right). \tag{11a}$$

The condition of the continuity of the perturbation depth on the interface is $\hat{h}(1^-) = -FU/G$, or

$$\Phi(1) = 0. \tag{11b}$$

This is equivalent to the condition of no flow normal to the interface, as can be seen from the first equation in (10); so we only have to find solutions of (10), that satisfy conditions (11a,b).

Solutions of the system (10) are limited by the presence of the inhomogeneous term

$$\frac{FU}{G}\bar{v}r,$$

which with the boundary condition (11b), results in a solvability condition for (10). The derivation of this solvability condition involves extensive algebra, which is not presented here, but the interested reader can obtain it by modifying Benilov's (1996) derivation for a similar system in his Eqs. (3.1)–(3.9). The solvability condition implies that there are no exact solutions of (10), unless the integrated mass anomaly $\iint (\bar{h} - 1) dx dy$ is zero; this does not occur for the typical oceanic eddies which have positive mass anomaly for anticyclones and negative for cyclones. This restriction prevents analytic consideration of the effects of a finite Coriolis force over a range of (F, G) using a complete system (10).

However, for oceanic eddies this inhomogeneous term can be very small. In particular, the ratio of its amplitude (rms) and the amplitude of the term $(\bar{h}\hat{v})$ in the third equation of (10) is $\sim F/(40G)$ for a particular velocity profile (9a) employed herein. For (F, G) corresponding to a typical Gulf Stream ring this ratio is about 0.015, and it can be much less if the eddy is smaller and/or closer to the equator. Let us consider neglecting this

inhomogeneous term and solve the corresponding homogeneous system:

$$\left. \begin{aligned} \left(\frac{\bar{v}\hat{v}}{r} + \hat{u} \frac{\partial \bar{v}}{\partial r} + \frac{\hat{u}\bar{v}}{r} \right) + F\hat{u} &= -G \frac{\Phi}{r} \\ \left(\frac{\bar{v}\hat{u}}{r} + \frac{2\bar{v}\hat{v}}{r} \right) + F\hat{v} &= G \frac{\partial \Phi}{\partial r} \\ \frac{\partial}{\partial r}(r\bar{h}\hat{u}) + \bar{h}\hat{v} + \Phi\bar{v} &= 0 \end{aligned} \right\}, \quad r < 1. \quad (12)$$

It should be understood that the approximation (12) will be valid only for a finite period of time $O(40GF^{-1})$ (which may be sufficiently large, as will be shown below in section 6).

It is easy to verify that a solution $\{\hat{u}_g, \hat{v}_g, \Phi_g\}$ of (12) is also an alpha-gyre [similar to (8a)]:

$$\left. \begin{aligned} \hat{u}_g &= -\alpha \frac{\bar{v}}{r} \\ \hat{v}_g &= \alpha \frac{\partial \bar{v}}{\partial r} \\ \Phi_g &= \alpha \frac{\partial \bar{h}}{\partial r} \end{aligned} \right\}, \quad r < 1. \quad (13a)$$

Since $\bar{v}(1) = 0$, from the first and the last equation of (13a) it is apparent that (13a) already satisfies the condition (11b) of no flow normal to the interface, and (11a) will also be satisfied for any given U if

$$\alpha \frac{\partial \bar{v}}{\partial r} \Big|_{r=1} = U \left[1 + \frac{K_0\left(\frac{1}{R_d}\right) + K_2\left(\frac{1}{R_d}\right)}{2R_d K_1\left(\frac{1}{R_d}\right)} \right]. \quad (13b)$$

The quasigeostrophic exterior is

$$\left. \begin{aligned} \hat{h}(r) &= -\frac{FU}{G} \frac{K_1\left(\frac{r}{R_d}\right)}{K_1\left(\frac{1}{R_d}\right)} \\ \hat{v}(r) &= U \left[1 + \frac{K_0\left(\frac{r}{R_d}\right) + K_2\left(\frac{r}{R_d}\right)}{2R_d K_1\left(\frac{1}{R_d}\right)} \right] \\ \hat{u}(r) &= U \left[-1 + \frac{K_1\left(\frac{r}{R_d}\right)}{rK_1\left(\frac{1}{R_d}\right)} \right] \end{aligned} \right\}, \quad r > 1. \quad (13c)$$

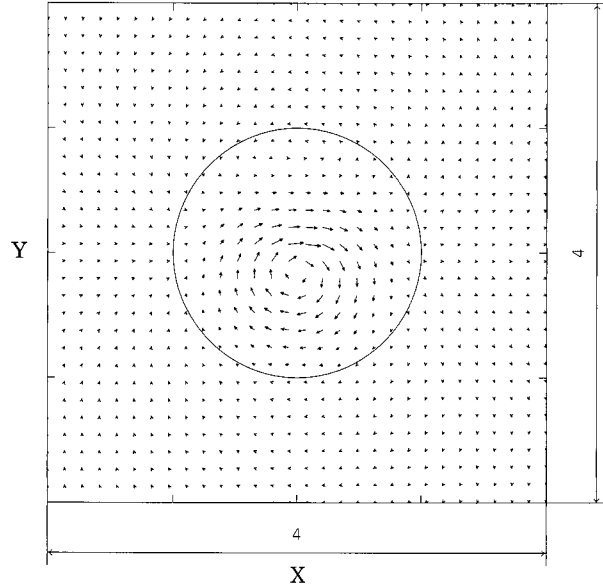


FIG. 3. Velocity field in the “alpha-gyre” eddy (see sec. 5) with $G = 30, F = 6$. The inner part of the eddy is almost uniformly shifted by a small amount in y direction with respect to the vortex boundary (thin solid line). The velocity field is dominantly monopolar, but there is a small (barely visible) counterflow just above the vortex, which occurs due to the small dipolar component.

Thus, the homogeneous problem can be solved for *any* (F, G) and any basic velocity profile that has zero velocity and nonzero vorticity at the edge. The total analytical solution (4) in which perturbation field is given by (13a,b,c) for $(F, G) = (6, 30)$ and $U = 0.1$ is presented in Figs. 3, 4. From these figures we can see the alpha-gyre signature of our solution: the interior field is almost uniformly shifted in the y direction with respect to symmetric exterior (the $r = 1$ boundary of the eddy is presented by the thin solid line). Note that Fig. 3 presents velocities in the stationary coordinate system.

Since the only difference between (10) and (12) is in the presence of the inhomogeneous term

$$-\frac{FU}{G} \bar{v}r$$

in the third equation of (10) we tentatively conclude that the eddies with relatively small values of

$$T = \frac{F}{G} = \frac{fv_{\max}R}{g'H}$$

are capable of moving a significant distance from the origin (even though this motion is expected to be time dependent). This assumption will be tested next by the numerical calculations.

6. Numerical calculations for the finite f case

For numerical integration in this section we used two different methods: the finite difference method of the

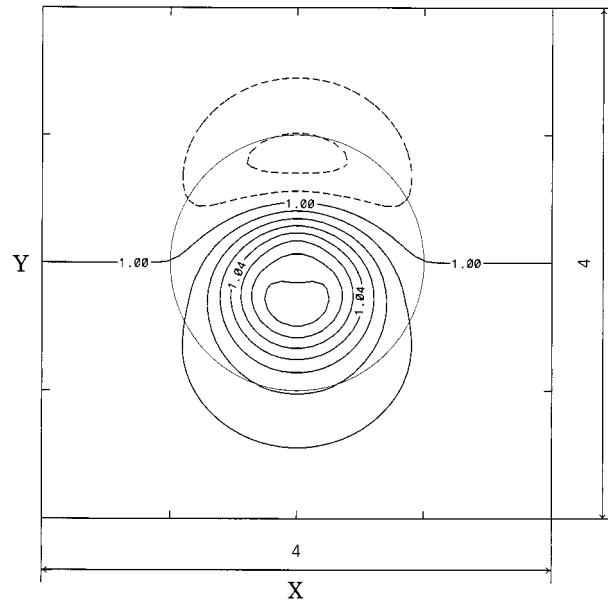


FIG. 4. Isopleths of the upper-layer thickness for the alpha-gyre eddy in Fig. 3. The solid contour lines correspond to the depression of the density interface ($h > 1$), and the dashed contour lines correspond to its elevation ($h < 1$). This anticyclonic eddy has clearly positive overall "mass anomaly" (see the text). The vortex is moving to the right.

Bleck and Boudra type (described in section 4), and a completely dealiased pseudospectral method in which all the equations (1) are inverted exactly in the Fourier space (assuming doubly periodic boundary conditions). Integration in time is performed by a fourth-order Runge-Kutta scheme. Both methods qualitatively agree in representing the evolution of eddies. Clear superiority of the spectral method was revealed when various high-order tests of accuracy were made. For instance, it could be shown by slightly modifying Ball's (1963) integral theorems that the components of integrated momentum on an f plane (with periodic boundary conditions) should oscillate harmonically at the inertial frequency ($2\pi F^{-1}$). These oscillations are nearly perfectly represented in the spectral model with a relative error in the absolute value of integrated momentum $\sim 10^{-8}$. The behavior of the "centroid of mass anomaly" (see below) is also in good agreement with the analytical prediction. The results presented in this section are therefore given for the spectral calculations using a 256×128 grid with $\Delta x = \Delta y = 0.08$, $\Delta t = 4 \times 10^{-3}$.

The numerical experiments were initiated with eddies perturbed by the alpha-gyre disturbances (13a,b,c) for $U = 0.1$; the basic velocity is (again) given by (9a) for cyclonic eddies, and for anticyclones it is

$$\bar{v} = -8.65r(1 - r) \exp(-2r), \quad r < 1. \quad (14)$$

The corresponding basic thickness is computed from the cyclostrophic balance (3). The resulting trajectories of the eddies with different values of (F, G) are shown in

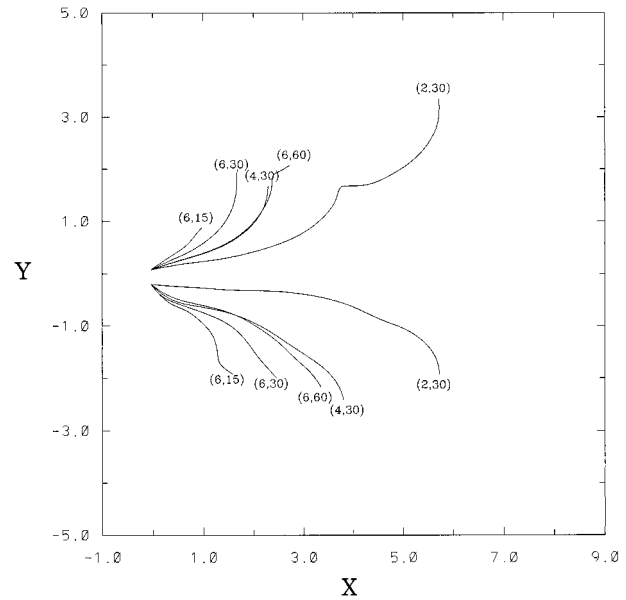


FIG. 5. Trajectories of the alpha-gyre vortices for the various values of the parameters (F, G) . The trajectories of the cyclonic eddies could be distinguished from the trajectories of the anticyclones by the fact that the former start from the point with slightly positive y and the latter originate from slightly negative y . The ageostrophic eddies (small F) are able to propagate much farther than the relatively geostrophic ones (large F).

Fig. 5. The coordinates of the center have been determined by the maximum deflection $|h - 1|$ of the density interface, and the computed initial propagation velocity was found to be close to the theoretical speed ($U = 0.1$). Each integration was stopped when either the translational velocity was reduced by a factor of 2 or the direction of the propagation changed by 90° . The trajectories of the cyclonic eddies in Fig. 5 are distinguished from the trajectories of the anticyclones by the fact that the former start from the point with slightly positive y and turn to the left and the latter originate from the slightly negative y and turn to the right.

The most important effect revealed in Fig. 5 is that the maximum propagation distance depends strongly on F ; the smaller F (ageostrophic vortices), the farther eddies propagate. For fixed F (see the eddies with $F = 6$ and various G in Fig. 5) the vortices with larger G (smaller Froude number) propagate farther. Note that the criterion of propagation from the previous section, namely the small values of $T = F/G$ (which is formally only a sufficient condition for propagation), appears to be directly related to the maximum separation of eddies from their origin: the eddies with small values of T in Fig. 5 move farther than the eddies with large T . The only exception from this in Fig. 5 is the anticyclone with $(F, G) = (4, 30)$ that moved slightly farther than the $(F, G) = (6, 60)$ eddy.

The reason why the geostrophic (large F) eddies do not propagate as far as the ageostrophic (small F) vortices becomes apparent from Ball's (1963) general the-

orem concerning the finite motion of a shallow rotating liquid. Ball derived equations of motion for the centroid of the fluid contained in a paraboloid, however, his derivation can be easily extended to consider the isolated eddy in an f -plane shallow-water $1\frac{1}{2}$ -layer model. In our case the term “centroid” will refer to the vertical displacement $(h - 1)$ of the density interface. Ball’s equations imply that the centroid should move in a circle with an inertial period of $2\pi f^{-1}$. [The case when the horizontally integrated value of the vertical displacement of the interface $(h - 1)$ vanishes identically is certainly an exception from Ball’s theorem; but this case, as was mentioned above, will not be considered here because of its limited relevance to oceanic eddies.]

Our calculations in Fig. 5 clearly demonstrate that, when the experiments are initiated by the compact vortices with finite mass anomaly, the eddies do not oscillate around the origin but propagate several radii, monotonically (in time) increasing their separation from the origin. This means that in the course of time the centroid over all the (x, y) plane and the more relevant “center” of an eddy (as defined, for example, by the pressure extremum) become separated by a large distance. Such a separation can occur only if by the end of our experiment the contribution to the coordinates of the centroid from the small irregular motions in the exterior field is (at least) comparable in absolute value to the contribution from the eddy interior ($r < 1$). A fast redistribution of thickness in the shallow-water model is accomplished by the small (in amplitude) but dynamically important inertia-gravity waves. These are not permitted when the Rossby number is small and the motion is effectively quasigeostrophic. In this case the eddy is kinematically bound to the centroid,¹ which explains why the relatively geostrophic (large F) eddies in Fig. 5 move less far from the origin than the ageostrophic (small F) ones do.

In order to confirm our suggestion that the redistribution of the height is accomplished mostly by the small amplitude gravity waves we performed the following diagnostics of the numerical calculations for the $(F, G) = (6, 30)$ anticyclone in Fig. 3. The thin solid line in Fig. 6 is the x coordinate of the centroid of interfacial displacement

$$C(t) = \frac{\iint (h - 1)x \, dx \, dy}{\iint (h - 1) \, dx \, dy}, \tag{15}$$

¹ It should be noted though that, in principle, even in the quasi-geostrophic case it is not impossible for the “center” of an eddy to become significantly separated from the centroid by the filamentation or by the evolution in some more complex way. However, the numerical calculations (Radko and Stern 1999) indicate that this separation is quite small when the integrated mass anomaly is finite.

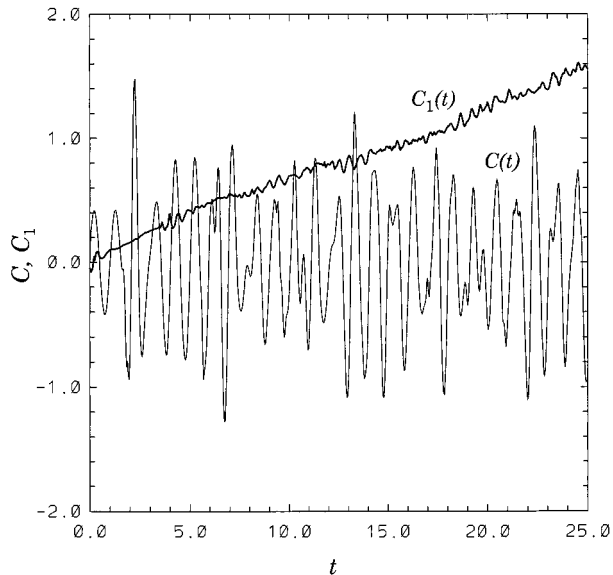


FIG. 6. The x coordinate of the centroid of mass anomaly $C(t)$ for the $(F, G) = (6, 30)$ eddy. This centroid exhibits oscillations around the vortex origin at approximately inertial frequency. When the contribution to the coordinates of the centroid from the small amplitude ($|h - 1| < 0.02$) gravity waves is filtered out (see the text), the resulting quantity $C_1(t)$ behaves in a completely different way. This proves that the observed separation between the centroid and the eddy itself is accomplished by the small amplitude inertia-gravity waves.

obtained from the numerical calculations. According to the analytical arguments (Ball 1963), $C(t)$ should perform harmonic oscillations with a period $(2\pi/F)$ as long as the value of $(h - 1)$ at the edge of the considered domain is close to zero [for infinite domains the corresponding condition is $|h - 1| \leq O(r^{-2})$], and curve $C(t)$ in Fig. 6 indeed oscillates at the (approximately) inertial frequency. Note the remarkably regular (sinusoidal) first period of oscillation ($0 < t < 1.5$), which is followed by the more irregular oscillations. The reason for this change is due to the gravity waves excited by the moving eddy (initially located at the center of computational domain). The speed of these waves ($\sim \sqrt{G}$) is such that it takes them about 1.5 units of time to reach the boundary of the domain and slightly modify the condition of Ball’s theorem [zero $(h - 1)$ at the boundary].

In the same figure we plotted the quantity,

$$C_1(t) = \frac{\iint_{|h-1|>0.02} (h - 1)x \, dx \, dy}{\iint_{|h-1|>0.02} (h - 1) \, dx \, dy}, \tag{16}$$

which is the same as (15) except that the integration is carried not over the all (x, y) computational domain, but over a part of it where the departure of h from its far-

field value exceeds 0.02. In other words, (16) is also a centroid but without the contribution to its x coordinate from the very small (linear) perturbations ($|h - 1| < 0.02$). From Fig. 6 it is apparent that such a filtering of these small gravity waves completely changes the qualitative and quantitative behavior of the centroid: $C(t)$ oscillates around the origin while $C_1(t)$ moves away from it. Even when only the perturbations with $|h - 1| < 0.01$ are similarly filtered out in (15), the resulting centroid (not shown) also moves away from the center, but slightly ($\sim 10\%$) slower and less regularly than $C_1(t)$. This means that the aforementioned redistribution of the interface is accomplished by the very small (and barely visible), but fast and therefore important, inertia-gravity waves. [Note also that in order to contribute to the separation between the centroid and the more relevant eddy center these waves do not have to actually transport mass since the centroid is a first moment of $(h - 1)$; therefore the shape of these perturbations is more important than the transported volume.]

The significance of the well-known and often used integral theorems may be even more limited in the real ocean where the other factors can contribute the separation between the centroid and the more relevant measures of eddy center. The potentially important effects (which are completely absent in the foregoing simple $1\frac{1}{2}$ -layer f -plane model) include the Rossby waves, various modes of internal waves, effects of finite ocean depth, etc. In order to demonstrate how the effects of a finite depth may enhance the self-propagating ability of eddies we will now present an analytical linear solution similar to those given in sections 3 and 5 but for a fully baroclinic model.

7. Self-propagation of eddies in a stratified fluid of finite depth

In order to examine the possibility of the *self-propagation* in a more generally stratified model we consider a quasigeostrophic f -plane rigid-lid approximation. For simplicity we shall consider the case of two active layers, but the derivation can easily be extended to the general case of n layers. The conservation of potential vorticity in each layer requires that

$$\left\{ \frac{\partial}{\partial t} - \frac{\partial \psi_n}{\partial y} \frac{\partial}{\partial x} + \frac{\partial \psi_n}{\partial x} \frac{\partial}{\partial y} \right\} Q_n = 0,$$

where $Q_n = \Delta \psi_n + (-1)^n (\psi_1 - \psi_2) F_n$ is the quasigeostrophic potential vorticity; ψ_n is the streamfunction in layer $n = 1, 2$; and F_n is the rotational Froude number in layer n . Here the equations are again nondimensionalized by the eddy radius and advective velocity. Let \bar{u}_n denote the basic velocity in layer n and assume that the velocity field in the exterior is irrotational and barotropic.

After rewriting the equations of motion in the frame of reference moving with speed U , and assuming that

vorticity interface propagates without change of shape, the irrotational exterior streamfunction is

$$\psi_1 = \psi_2 = U(r - 1/r) \sin \theta.$$

The details of the derivation of the linearized interior vorticity equation are similar to those in the barotropic case solved by (SR), and the result is

$$\bar{u}_1(r) \frac{\partial}{\partial \theta} \{ \Delta \psi'_1 + F_1(\psi'_2 - \psi'_1) \} - \frac{\partial}{\partial \theta} \{ \psi'_1 \} \frac{\partial}{\partial r} \{ \Delta \bar{\psi}_1 + F_1(\bar{\psi}_2 - \bar{\psi}_1) \} = 0 \quad (17)$$

$$\bar{u}_2(r) \frac{\partial}{\partial \theta} \{ \Delta \psi'_2 + F_2(\psi'_1 - \psi'_2) \} - \frac{\partial}{\partial \theta} \{ \psi'_2 \} \frac{\partial}{\partial r} \{ \Delta \bar{\psi}_2 + F_2(\bar{\psi}_1 - \bar{\psi}_2) \} = 0 \quad (18)$$

$$\psi'_n(1) = 0, \quad \frac{\partial}{\partial r} \psi'_n(1) = 2U \sin \theta,$$

$$n = 1, 2 \quad (19)$$

where $\bar{\psi}_n$ denotes the basic and ψ'_n the perturbation streamfunctions in layer n . Equations (17)–(19) have a separable solution $\Psi'_n = A \Phi_n(r) \sin \theta$, where

$$\bar{u}_1 \left\{ \Phi''_1 + \frac{1}{r} \Phi'_1 \right\} - \Phi_1 \left\{ \bar{u}'' + \frac{1}{r} \bar{u}' \right\} = F_1(\bar{u}_2 \Phi_1 - \bar{u}_1 \Phi_2),$$

$$\bar{u}_2 \left\{ \Phi''_2 + \frac{1}{r} \Phi'_2 \right\} - \Phi_2 \{ \bar{u}_2'' + u_2' \} = F_2(\bar{u}_1 \Phi_2 - \bar{u}_2 \Phi_1),$$

$$\Phi_n(1) = 0,$$

$$A \Phi'_n(1) = 2U.$$

From these equations it follows that if $\bar{u}'_1(1^-) = \bar{u}'_2(1^-)$; that is, if the baroclinic vorticity at the edge of the eddy vanishes, then an $m = 1$ disturbance resulting in the rectilinear (to the leading order) translation of the entire eddy can be found:

$$\Phi_n = \bar{u}_n(r) \quad \text{for } r < 1; \quad A = \frac{2U}{\bar{u}'_n(1)},$$

$$n = 1, 2; \quad \bar{u}'_1(1^-) = \bar{u}'_2(1^-). \quad (20)$$

This solution is very similar to the eddy in section 3 since it consists of a uniformly shifted interior ($r < 1$) and irrotational dipolar exterior. The physical explanation of the rectilinear propagation of this vortex is as follows. In each layer the alpha-gyre disturbance (20) shifts the interior structure of the vortex in the y direction (providing the dipolar moment for the propagation). Moreover, the displacement of the interior streamlines ($\delta y = A = 2U/\bar{u}'_n(1)$) is the same in both layers because of the assumption that the vorticity jumps are equal. So the balanced structure of the symmetric vortex will remain balanced in the interior (though slightly shifted)

up to the second order after we introduce this alpha-gyre disturbance.

Spectral calculations (not presented here) were performed for such eddies with a basic velocity of the form

$$u_i(r) = C_i r(1 - r) \exp(-\alpha_i r),$$

$$r < 1, \quad i = 1, 2$$

for various values of C_i and α_i (satisfying the requirement of a zero baroclinic vorticity jump at the edge). The objective of those calculations was to see how robust the finite amplitude structure would be. Although the vortex moved initially with the predicted velocity, after it traveled a distance comparable to its diameter a rapid destruction of the initial form followed. This was considered to be the consequence of an instability of the baroclinic modes. The stability of circular vortices in the baroclinic model was examined by Gent and McWilliams (1986) for several velocity profiles. They showed that the vortices in a stratified fluid (and in particular the baroclinic $m = 1$ modes) are very likely to be strongly unstable. However, there is no reason to assume that the system of two coaxial vortices is unstable for all velocity profiles, and ample evidence from observations of the existence of long-lived vortices in the ocean strongly supports this conclusion. Therefore, the possibility of the existence of robust propagating quasi-monopolar structures in the two-layer model should be considered in the future.

To demonstrate the general character of the alpha-gyre solution let us obtain a similar solution in the quasi-geostrophic model with continuous stratification. The potential vorticity is now

$$Q = \Delta\psi + \frac{1}{\bar{\rho}} \frac{\partial}{\partial z} \bar{\rho} \frac{f^2}{N^2} \frac{\partial}{\partial z} \psi,$$

where Ψ is the streamfunction, $\bar{\rho}(z)$ is the density, and $N(z)$ is the Brunt-Väisälä frequency. In the moving coordinate system, conservation of the quasigeostrophic potential vorticity and the condition of the stationary solution will require

$$J\left(\psi, \Delta\psi + \frac{1}{\bar{\rho}} \frac{\partial}{\partial z} \bar{\rho} \frac{f^2}{N^2} \frac{\partial}{\partial z} \psi\right) = 0. \quad (21)$$

Let us adopt the barotropic solution, $\psi = U(r - 1/r) \sin\theta$, for the exterior region. Equation (21) linearized in the interior can be written as

$$\bar{u} \frac{\partial}{\partial \theta} \left\{ \Delta\psi' + \frac{1}{\bar{\rho}} \frac{\partial}{\partial z} \bar{\rho} \frac{f^2}{N^2} \frac{\partial}{\partial z} \psi' \right\}$$

$$- \frac{\partial}{\partial \theta} \psi' \frac{\partial}{\partial r} \left\{ \bar{u}' + \frac{1}{r} \bar{u} + \frac{1}{\bar{\rho}} \frac{\partial}{\partial z} \bar{\rho} \frac{f^2}{N^2} \frac{\partial}{\partial z} \bar{u} \right\} = 0,$$

and variables can be separated by $\psi' = A\Phi(r, z) \sin\theta$. The resulting differential equation

$$\bar{u} \left\{ \Phi'' + \frac{1}{r} \Phi' \right\} - \Phi \left\{ \bar{u}'' + \frac{1}{r} \bar{u}' \right\} + \bar{u} \frac{1}{\bar{\rho}} \frac{\partial}{\partial z} \bar{\rho} \frac{f^2}{N^2} \frac{\partial}{\partial z} \Phi$$

$$- \Phi \frac{1}{\bar{\rho}} \frac{\partial}{\partial z} \bar{\rho} \frac{f^2}{N^2} \frac{\partial}{\partial z} \bar{u} = 0 \quad (22)$$

with the boundary conditions $\Phi(1, z) = 0, A\Phi_r'(1, z) = 2U$ allows for the alpha-gyre solution:

$$\Phi = \bar{u}(r, z), \quad A = \frac{2U}{\bar{u}'(1, z)}, \quad r < 1,$$

as long as $\bar{u}'(1, z) = \text{const.}^2$

Note that the propagating solutions in this section are obtained without any approximations (in addition to the basic assumption that the $m = 0$ mode is dominant), unlike the eddies in the model with the deep and passive lower layer (sec. 5).

8. Conclusions

We have shown (sec. 6) that the quasi-monopolar vortices in the shallow-water 1½-layer model are able to translate over large distances without the β effect, but only due to the presence of a small dipolar moment. The ageostrophic eddies propagate much farther than the vortices with small values of Rossby number (F^{-1}), and the numerical calculations indicate that the maximum distance of propagation (in units of eddy radius) depends on the nondimensional number

$$T = \frac{fv_{\max}R}{g'H}.$$

However, when the effects of finite depth are included (sec. 7) we analytically show that the geostrophic eddies also may be capable of *self-propagation*. The eddies can propagate over the distances much larger than their radius even in the nonrotating systems (sections 3, 4). All the presented solutions have a distinctive “alpha-gyre” signature, such that the interior of eddies is almost uniformly shifted (with respect to the symmetric dipolar exterior field) by a small amount in the direction normal to the direction of motion.

In connection with the ability of an eddy to propagate for a significant period of time with the velocity determined by its initial dipolar moment we remark that the oceanic eddies propagate with velocities that often differ from the theoretical predictions, some eddies move up to five times faster than required by the beta effect. The effect of a large-scale mean motion does not always appear to be sufficient to explain the difference (Chassignet et al. 1990). The direction of propagation also

² Reference should also be made to Flierl’s (1988) normal mode calculation for the two-layer quasigeostrophic eddies with piece-wise uniform vorticity. He showed that the $m = 1$ circular Fourier mode is degenerate, which implies the possibility of rectilinear propagation of the vortex.

does not always correspond to the beta-induced westward drift. Our results may help to explain the aforementioned observations by the presence of a small dipolar moment, which may not be related to beta effect.

REFERENCES

- Ball, F. K., 1963: Some general theorems concerning the finite motion of a shallow rotating liquid lying on a paraboloid. *J. Fluid Mech.*, **17**, 240–256.
- Benilov, E. S., 1996: Beta-induced translation of strong isolated eddies. *J. Phys. Oceanogr.*, **26**, 2223–2229.
- Bleck, R., and D. B. Boudra, 1986: Wind-driven spin up in eddy resolving ocean models formulated in isopicnic and isobaric coordinates. *J. Geophys. Res.*, **91**, 7611–7621.
- Chassignet, E. P., D. B. Olson, and D. B. Boudra, 1990: Motion and evolution of oceanic rings in a numerical model and in observations. *J. Geophys. Res.*, **95**, 22 121–22 140.
- Flierl, G. R., 1988: On the instability of geostrophic vortices. *J. Fluid Mech.*, **197**, 349–388.
- , V. D. Larichev, J. C. McWilliams, and G. M. Reznik, 1980: The dynamics of baroclinic and barotropic solitary eddies. *Dyn. Atmos. Oceans*, **5**, 1–41.
- Gent, P. R., and J. C. McWilliams, 1986: The instability of barotropic circular vortices. *Geophys. Astrophys. Fluid Dyn.*, **35**, 209–233.
- Killworth, P. D., 1983: On the motion of isolated lenses on a beta-plane. *J. Phys. Oceanogr.*, **13**, 368–376.
- , 1986: On the propagation of isolated multilayer and continuously stratified eddies. *J. Phys. Oceanogr.*, **16**, 709–716.
- Larichev, V. D., and G. M. Reznik, 1976: Two-dimensional solitary Rossby waves. *Dokl. Akad. Nauk SSSR*, **231**, 1077–1079.
- Nof, D., 1983: On the migration of isolated eddies with application to Gulf Stream rings. *J. Mar. Res.*, **41**, 399–425.
- Nycander, J., and G. G. Sutyrin, 1992: Steadily translating anticyclones on the beta-plane. *Dyn. Atmos. Oceans*, **16**, 473–498.
- Radko, T., and M. E. Stern, 1999: On the propagation of oceanic mesoscale vortices. *J. Fluid Mech.*, **380**, 39–57.
- Stern, M. E., and T. Radko, 1998: The self propagating quasi-monopolar vortex. *J. Phys. Oceanogr.*, **28**, 22–39.